Robust Design of Countercurrent Adsorption Separation: 3. Nonstoichiometric Systems

Marco Mazzotti
Dipartimento di Chimica, Politecnico di Milano, 20131 Milano, Italy

Giuseppe Storti
Dipartimento di Ingegneria Chimica e Materiali, Università degli Studi di Cagliari, 09123 Cagliari, Italy

Massimo Morbidelli
Laboratorium für Technische Chemie LTC, ETH Zentrum, Universitätstrasse 6, CH-8092 Zürich, Switzerland

The separation of a multicomponent mixture in a countercurrent adsorptive separation unit is analyzed. A procedure for the optimal and robust design of the operating conditions of the unit is developed in the frame of equilibrium theory, where the adsorption equilibria are described through the constant selectivity nonstoichiometric Langmuir model, while mass-transfer resistances and axial dispersion are neglected. This allows for extending the results previously obtained for systems characterized by either the linear or stoichiometric Langmuir isotherm to cases where the adsorbates exhibit rather different loading capacities. Analogies and differences among these three equilibrium models with respect to the criteria for the choice of operating conditions of countercurrent separation units are discussed. A comparison between model predictions and experimental data assesses the reliability and accuracy of the theoretical results achieved in this work.

Introduction

Continuous true countercurrent (TCC) units can be used for the adsorptive separation of multicomponent mixtures (cf. Ruthven, 1984; Ganetsos and Barker, 1993). In practical applications the countercurrent contact between the fluid and the solid phases is accomplished in a simulated fashion, by keeping the solid beds fixed and moving periodically the locations of the inlet and outlet ports in the same direction of the fluid stream. This is the simulated moving bed (SMB) configuration, whose classical applications include xylenes in liquid (Broughton and Gerhold, 1961; Johnson and Kabza, 1993) and vapor phase (Storti et al., 1992, 1993b), linear/nonlinear paraffins in liquid (Ruthven and Ching, 1989; Johnson and Kabza, 1993) and vapor phase (Baciocchi et al., 1996), sugars (cf. Ruthven and Ching, 1989), enantiomers (Negawa and Shoji, 1992; Ching et al., 1993; Nicoud et al., 1993) and others.

With reference to the typical scheme of a TCC unit shown in Figure 1, both TCC and SMB units allow a single cut of a multicomponent feed stream. Using a desorbent stream to regenerate the adsorbent, complete separation is sought, where the most and the least adsorbable components of the feed are collected in the extract and in the raffinate stream, respectively.

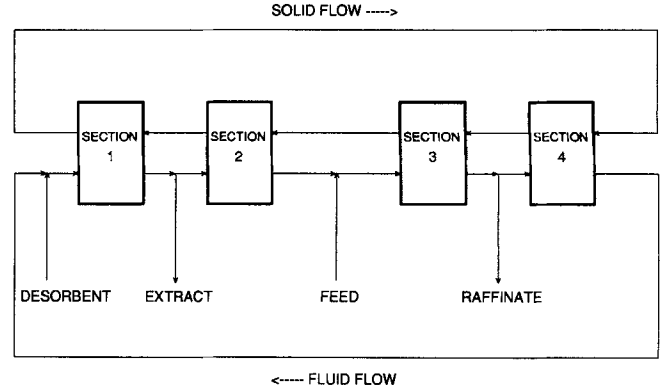

Figure 1. Four-section closed-loop true countercurrent unit for adsorption separation.

Correspondence concerning this article should be addressed to M. Morbidelli.

With the objective of achieving the requirement of complete separation, the correct choice of the operating conditions of countercurrent separation units is of key importance. Thanks to the accepted equivalence between TCC and SMB units (Ruthven and Ching, 1989), the former has been extensively used for the optimal design of the latter. On the one hand, operating conditions can be selected by approximating the unit as a sequence of equilibrium stages and applying a McCabe-Thiele-like analysis (Ruthven, 1984; Hashimoto et al., 1993). On the other hand, a different approach is based on the equilibrium theory model, where axial mixing and mass transport resistances are neglected, solid flow rate, solid density, external and intraparticle void fraction are constant, and adsorption equilibrium is assumed to be established everywhere at every time in the column. In this frame, the model equations of the j-th section of the TCC unit in Figure 1 are given by the following set of first-order partial differential equations

$$\frac{\partial}{\partial \tau}\left[\epsilon^* y_i^j + (1-\epsilon^*)\sigma\theta_i^j\right] + (1-\epsilon_p)\,\sigma\frac{\partial}{\partial x}\left[m_j y_i^j - \theta_i^j\right] = 0 \qquad (i=1, \ldots, NC), \quad (1)$$

where

$$\theta_i^j = f_i^{eq}(\mathbf{y}^j) \qquad (i=1, \ldots, NC). \quad (2)$$

The boundary conditions are given by

$$\begin{aligned} y_i^j(\tau,0) &= (y_i^j)^a \qquad (i=1, \ldots, NC)\\ \theta_i^j(\tau,1) &= (\theta_i^j)^b \qquad (i=1, \ldots, NC)\\ y_i^j(0,x) &= (y_i^j)^o \qquad (i=1, \ldots, NC) \end{aligned} \quad (3)$$

In particular $y_i = c_i/\rho_f$ and $\theta_i = \Gamma_i/\Gamma^\infty$ represent dimensionless fluid and adsorbed phase concentrations, respectively, and are defined through constant reference values of the fluid molar density ρ_f and the adsorbed concentration Γ^∞.

From inspection of the equations above, it is readily seen that for a given system characterized by a specific adsorption equilibrium model (Eq. 2), the steady-state behavior of the countercurrent unit is determined only by the values of the flow rate ratios m_j. These are defined as the ratio between the net fluid flow rate and the adsorbed-phase flow rate in each section of the unit

$$m_j = \frac{\text{net fluid flow rate}}{\text{adsorbed phase flow rate}} = \frac{u_j\rho_f - u_s\epsilon_p\rho_f}{u_s\rho_s\Gamma^\infty(1-\epsilon_p)}. \quad (4)$$

The parameters m_j are constant values if the fluid-phase velocities u_j are constant. It follows that in the framework of the equilibrium theory the design problem for countercurrent units reduces to developing criteria for the optimal choice of the values of the m_j parameters.

In parts 1 and 2 of this series (Storti et al., 1993a; Mazzotti et al., 1994), optimal design criteria have been developed for systems described by the linear adsorption isotherm $\Gamma_i = H_i c_i$ and by the constant selectivity stoichiometric Langmuir isotherm

$$\theta_i = \frac{\Gamma_i}{\Gamma^\infty} = \frac{K_i y_i}{\sum_{l=1}^{NC} K_l y_l}, \quad (5)$$

including both binary and multicomponent systems.

These criteria provide the boundaries of the complete separation region in the space spanned by the four operating parameters m_j, with $j=1, \ldots, 4$. This is the region constituted of operating points for which both the extract and the raffinate achieve 100% purity, i.e., strong and weak components are collected in the extract and raffinate, respectively, and do not end up in the other outlet stream. Projecting this region onto the plane (m_2, m_3) yields a characteristic triangle shaped region, whose internal points correspond to operating conditions which in the frame of equilibrium theory lead to complete separation (see Figure 2). This graphical representation has proved to be very effective, since several features of the separation can be easily analyzed for different operating conditions in the (m_2, m_3) plane. In particular, robust and operating conditions can be easily determined (Storti et al., 1993a). Moreover, beside the complete separation region three more regions in the (m_2, m_3) plane can be determined; two of them correspond to operating conditions characterized by only one outlet stream pure, and the last one corresponds to operating conditions where neither outlet stream is pure (see Figure 2) (Storti et al., 1995). It is worth noting that several robust and optimal design considerations (in terms of disturbances, purity of the outlet streams, recovery of the feed components, desorbent and adsorbent requirement and productivity) are based on the shape of the complete separation region, and do not necessarily require its exact position in space.

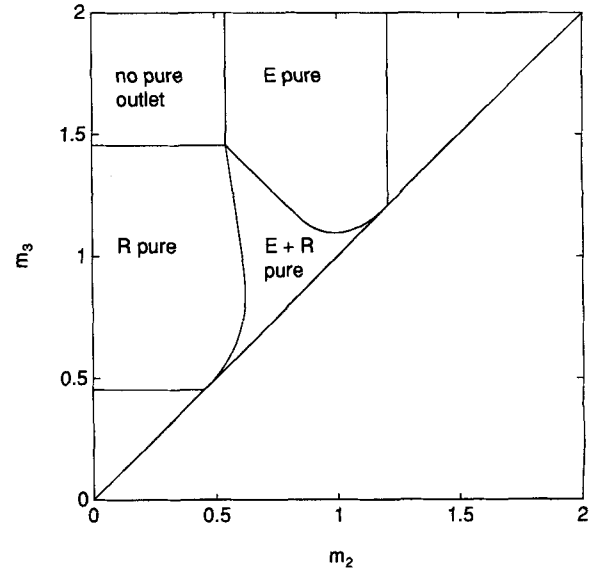

Figure 2. Regions of the (m_2, m_3) plane with different separation regimes in terms of purity of the outlet streams for a system described by the stoichiometric Langmuir isotherm: $y_A^F = y_B^F = 0.5$, $K_A = 2.67$, $K_B = 1$, $K_D = 2.21$.

Linear isotherms are of modest practical interest (mainly confined to dilute systems), whereas stoichiometric Langmuir isotherms can describe various systems of applicative interest, such as the alkyl-aromatic C_8 fraction on zeolites. In the case of the latter isotherm it is assumed that all the adsorbates have the same saturation loading capacity Γ^∞ and their adsorptivity is so high that the adsorbent solid is always saturated. Whatever the composition of the fluid phase is, the total coverage equals one, i.e., $\Theta = \sum_{i=1}^{NC} \theta_i = 1$.

However, in some instances these assumptions are not fulfilled since the adsorbates exhibit rather different loading capacities, as for example in the case of the separation of linear (high loading capacity) and nonlinear (low loading capacity) paraffins on 5A-Zeolite (Barrer, 1978). In these cases the constant selectivity nonstoichiometric Langmuir isotherm can be used

$$\theta_i = \frac{\Gamma_i}{\Gamma^\infty} = \frac{(\Gamma_i^\infty/\Gamma^\infty)\, K_i c_i}{\delta} = \frac{(\Gamma_i^\infty/\Gamma^\infty)\rho_f K_i y_i}{\delta}, \qquad (6)$$

where

$$\delta = \delta_{LNS} = 1 + \sum_{l=1}^{NC} K_l c_l = 1 + \rho_f \sum_{l=1}^{NC} K_l y_l, \qquad (7)$$

and the subscript *LNS* refers to the nonstoichiometric Langmuir isotherm. It is worth noting that this model lacks of thermodynamic consistency and should be regarded merely as an empirical relationship which, on the other hand, has been proved useful in various instances of practical interest (Ruthven, 1984). The selectivity of component i with respect to component l is given as follows

$$S_{il} = \frac{\Gamma_i/\Gamma_l}{c_i/c_l} = \frac{\Gamma_i^\infty K_i}{\Gamma_l^\infty K_l} = \frac{\gamma_i}{\gamma_l}, \qquad (8)$$

where $\gamma_i = \Gamma_i^\infty K_i$.

The objective of this work is to extend the criteria for optimal design of countercurrent separation units to systems described by this kind of isotherm. With reference to a binary feed with a given selectivity between the two components to be separated, the outcome of the analysis will be twofold: on one hand it will be shown that the complete separation region predicted using the nonstoichiometric model (Eq. 6) may be quantitatively very different from that predicted by the stoichiometric model (Eq. 5). On the other hand, the overall features of the complete separation region and its dependence on such parameters as desorbent adsorptivity and feed composition are qualitatively the same as those demonstrated for stoichiometric systems. It follows that issues such as robust and optimal operating conditions can be dealt with in the same manner as discussed earlier by Storti et al. (1993a).

Equilibrium Theory

In this section we discuss the mathematical model of the countercurrent adsorptive separation unit shown in Figure 1 when the nonstoichiometric Langmuir isotherm (Eq. 6) is used to characterize the adsorption equilibria. First some remarks on the properties of the equilibrium model are made; then, the assumptions on which the equilibrium theory is based are critically discussed, and the complete model of the separation unit is presented.

Nonstoichiometric Langmuir isotherm

Beside different saturation loading capacities, the nonstoichiometric isotherm (Eq. 6) differs from the stoichiometric one (Eq. 5) for the presence of the unitary term in the denominator of Eq. 6, which makes the adsorbed-phase concentration dependent upon the overall fluid-phase density. This can be observed by considering Eq. 6 in the particular case where $\Gamma_i^\infty = \Gamma^\infty$, for every $i = 1, \ldots, NC$, which leads to total coverage lower then one, namely $\Theta = 1 - 1/\delta_{LNS}$. It is readily seen that the greater the fluid density ρ_f, the lower the fraction of free adsorption sites $1/\delta_{LNS}$.

It is worth noticing that the linear isotherm and the stoichiometric Langmuir isotherm can be seen as particular cases of the nonstoichiometric model (Eq. 6). In the linear case the denominator in Eq. 6 equals one, i.e., $\delta = \delta_L = 1$ where the subscript L refers to the linear isotherm, and all the parameters in the numerator are grouped in the Henry constant H_i. In the stoichiometric case, $\delta = \delta_{LS} = \rho_f \sum_{l=1}^{NC} K_l y_l$ (with the subscript *LS* indicating the stoichiometric Langmuir case) and $\Gamma_i^\infty = \Gamma^\infty$, for every $i = 1, \ldots, NC$. Therefore, the nonstoichiometric equation can be seen as the general case, from which the other two can be derived as special cases. The linear equation applies to very dilute systems, where the sum in the δ term can be neglected with respect to one (see Eq. 7). On the other hand, the stoichiometric relationship applies to mixtures whose components have the same saturation loading capacity and a high adsorptivity, i.e., high K_i values. In this case the ratio $\Gamma_i^\infty/\Gamma^\infty = 1$, the unit in Eq. 7 can be neglected and the relevant δ_{LS} parameter is obtained.

A final remark concerns the applicability of the nonstoichiometric adsorption isotherm (Eq. 6), which in general refers to the case of a mixture of *NC* adsorbable components. It also includes the special case where one of the components is nonadsorbable, i.e., the corresponding $K = 0$ in Eq. 6, as for example the separations studied by Rhee et al. (1971) where an inert solvent was used.

Equilibrium theory model of a countercurrent column

Equation 1 with the equilibrium relationship (Eq. 2) given by one of the isotherms considered above, together with the boundary conditions (Eq. 3), constitutes a set of first-order hyperbolic partial differential equations, which under the assumption of constant fluid-flow rate admit analytical solution (Helfferich and Klein, 1970; Rhee et al., 1971; 1989; Storti et al., 1989).

The solution in the linear case is trivial (Ruthven, 1984). In the case of the other two isotherms the solution procedure is based on the one-to-one mapping between the space of fluid- or adsorbed-phase concentrations, in equilibrium with each other, and the Ω space, whose components are obtained as roots of the equation

$$\sum_{i=1}^{NC} \frac{K_i \Gamma_i}{\gamma_i - \omega} = 1. \qquad (9)$$

Let NC be the number of adsorbable components in the fluid mixture. It is worth noticing that in the nonstoichiometric case the Ω space is a NC-dimensional space, whereas in the stoichiometric case it has only $(NC-1)$ dimensions, being one of the NC ω values identically zero.

An important aspect refers to the assumption of constant fluid velocity, which is a prerequisite for the existence of the analytical solution. If this were not the case, an analytical solution would exist only in very particular cases (cf. LeVan et al. (1988) for the case of monovariant systems and Filippov (1994) for the case of a multicomponent system characterized by linear equilibria). The reliability of this critical hypothesis requires some further comments.

Let us first remove the assumption of constant fluid-flow rate and derive a differential equation for it. Multiplying Eq. 1 by ρ_f/ρ_i and summing over all components yields the following equation in the unknown fluid phase velocity u

$$\frac{\partial u}{\partial x} = u_s \rho_s \Gamma^{\infty}(1-\epsilon_p)\left[\frac{\partial s}{\partial x} - (1-\epsilon)\frac{\partial s}{\partial \tau}\right] \tag{10}$$

where s is defined as

$$s = \frac{1}{\Gamma^{\infty}} \sum_{i=1}^{NC} \frac{\Gamma_i}{\rho_i}. \tag{11}$$

In deriving Eq. 10 the following actions have been taken: (1) the relationship (Eq. 4) between m and u, which involves only constant parameters, has been used; (2) the additivity of volumes has been assumed as mixing rule for the fluid phase; hence, the identity $\sum_{i=1}^{NC} c_i/\rho_i = 1$ has been used wherever necessary; (3) the sum yielding Eq. 10 is done over all the components of the fluid mixture, including the nonadsorbable solvent, if there is one. In this latter case the sum defining s in Eq. 11 includes a null term, namely the one corresponding to the solvent.

It is now apparent that the assumption of constant fluid-flow rate is rigorously fulfilled only if the righthand side of Eq. 10 is zero, i.e., when s is constant. In the case of the three equilibrium isotherms considered in this work, using Eq. 6 the following relationships for s are obtained

Linear isotherm

$$s_L = \frac{1}{\Gamma^{\infty}} \sum_{i=1}^{NC} \frac{H_i c_i}{\rho_i}. \tag{12}$$

Stoichiometric Langmuir isotherm

$$s_{LS} = \frac{\sum_{i=1}^{NC}(K_i c_i/\rho_i)}{\sum_{i=1}^{NC} K_i c_i}. \tag{13}$$

Nonstoichiometric Langmuir isotherm

$$s_{LNS} = \frac{\sum_{i=1}^{NC}(\Gamma_i^{\infty}/\Gamma^{\infty})(K_i c_i/\rho_i)}{1+\sum_{i=1}^{NC} K_i c_i}. \tag{14}$$

At this stage it is worth noting that in the case of vapor-phase adsorption ρ_f can be taken as the ideal gas law molar density, which is constant at constant temperature and pressure and equals the values of single component molar densities. In the case of liquid-phase adsorption in principle molar densities of different components are different, though in practice they are rather similar since adsorption separations involve rather similar chemical species. As a consequence in the following analysis we always assume that all components have the same molar density and this corresponds to the reference value ρ_f, i.e., $\rho_i = \rho_f$ for every $i = 1, \ldots, NC$. Therefore, ρ_f is also equal to the overall fluid-phase molar concentration.

In the linear case the parameter H_i is different for different components and in general neither s_L nor u are constant. However the linear model applies to dilute systems, where in fact $c_i \ll \rho_i$, with the single exception of the nonadsorbable solvent for which $H = 0$. Thus, in this case s is very small and its changes are also negligible. Therefore, the assumption of constant fluid flow rate is approximately correct even though it is not rigorously fulfilled.

In the case of the stoichiometric Langmuir isotherm, s_{LS} given by Eq. 13 equals $1/\rho_f$, which we have assumed to be constant; therefore, the fluid-flow rate is rigorously constant. Note that in this case the presence of a nonadsorbable solvent cannot be accounted for due to the assumption of constant saturation of the adsorbent.

As mentioned above, the nonstoichiometric Langmuir isotherm can reduce to either one of the other two isotherms under specific circumstances. In both these cases the assumption of constant fluid-flow rate can be justified as discussed above. However, in the general case, where the saturation loading capacities of the involved components are different, the parameter s_{LNS} changes and so does the fluid-flow rate along the column, particularly in the case of bulk separations. On the other hand, the existence of the analytical solution of the equilibrium theory model limits us to use nonstoichiometric equilibrium models but with constant velocity. Indeed, this is a rather useful approach which leads to a model with improved predictive capabilities with respect to the stoichiometric equilibrium model for a wide variety of systems. This will become apparent after the comparison with experimental results discussed later.

Equilibrium theory model of a countercurrent separation unit

In order to develop criteria for the choice of the operating conditions leading to complete separation two different approaches can be followed. The first one requires the solution of several *simulation* problems, i.e., the problem of determining the performance of the unit for given operating conditions, within a trial-and-error procedure until the design requirements are fulfilled. The second approach solves the *design* problem directly, i.e., the problem of determining the operating conditions leading to the desired separation performance. In both cases the proper operating conditions are the flow rate ratios m_j in the four sections of the unit.

The second approach has been adopted throughout. In particular, in the case of binary separations described by the stoichiometric Langmuir isotherm, explicit relationships for the boundaries of the complete separation region have been determined. On the other hand, for multicomponent separa-

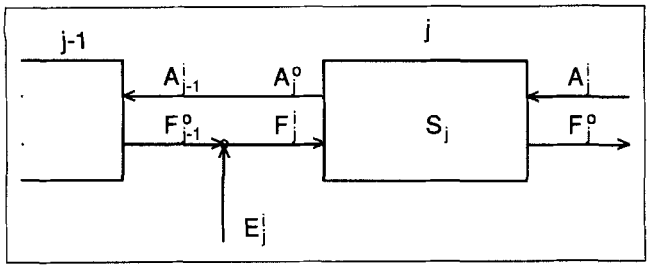

Figure 3. Generic *j*th section of a countercurrent adsorption unit.

tions, the direct approach must be complemented with a numerical procedure for searching the region of complete separation.

In the case of systems characterized by the nonstoichiometric Langmuir isotherm the first approach is more convenient, with the only exception of a binary mixture with a nonadsorbable desorbent, which will be dealt with in the Appendix. In order to apply this approach the *simulation* problem must be solved using the equilibrium theory model of the countercurrent separation unit. This model is constituted of one system of Eqs. 1 to 3 for each section of the unit, together with the proper material balances at the nodes of the unit (see Figure 1). The model equations are written assuming given operating conditions, i.e., known values of the flow rate ratios m_j in each section of the unit.

Equilibrium theory provides the time and space dependent analytical solution of the model of a single section of the countercurrent unit. With the aim of determining the separation performance of the unit, only the steady-state solution is needed and this is given by a constant state prevailing in each section, which depends only on the state of the two incoming streams and on the mass-flow rate ratio m_j in the section. With reference to Figure 3, let us indicate the steady constant state prevailing in section j by $\boldsymbol{S}_j$ and the states of the two incoming streams by $\boldsymbol{F}^i_j$ and $\boldsymbol{A}^i_j$, where the symbols $\boldsymbol{F}$ and $\boldsymbol{A}$ refer to the fluid and the adsorbed phase compositions, respectively. Correspondingly, the states of the two outgoing streams are represented by $\boldsymbol{F}^o_j$ and $\boldsymbol{A}^o_j$. Each section is preceded on the left by a node where fluid streams either mix with an external stream or split producing an external stream, which is indicated by $\boldsymbol{E}_j$. Therefore, there are six unknown states for each section of the unit, namely $\boldsymbol{S}_j$, $\boldsymbol{F}^i_j$, $\boldsymbol{A}^i_j$, $\boldsymbol{F}^o_j$, $\boldsymbol{A}^o_j$ and $\boldsymbol{E}_j$. If the operating parameters m_j, $j = 1, \ldots, 4$, are fixed these unknown states are determined by the following relationships, which constitute the equilibrium theory mathematical model of the entire countercurrent separation unit:

Equilibrium Theory Solution (Rhee et al., 1989)

$$\boldsymbol{S}_j = f_{ET}\left(\boldsymbol{F}^i_j, \boldsymbol{A}^i_j, m_j\right) \tag{15}$$

Material Balances at the Right and Left Section Ends (Rhee et al., 1989)

$$b\left(\boldsymbol{S}_j, \boldsymbol{F}^o_j, \boldsymbol{A}^i_j, m_j\right) = 0 \tag{16}$$

$$b\left(\boldsymbol{S}_j, \boldsymbol{F}^i_j, \boldsymbol{A}^o_j, m_j\right) = 0 \tag{17}$$

Specification of the External Stream, $\boldsymbol{E}_j$

$$\boldsymbol{E}_j = \text{known state}. \tag{18}$$

Material Balance at Node j on the lefthand side of section j

$$n\left(\boldsymbol{E}_j, \boldsymbol{F}^i_j, \boldsymbol{F}^o_{j-1}, m_j, m_{j-1}\right) = 0 \tag{19}$$

Continuity of the Solid Streams between the (j − 1)th and jth Sections

$$\boldsymbol{A}^i_{j-1} = \boldsymbol{A}^o_j. \tag{20}$$

The above equations must be written for $j = 1, \ldots, 4$ and, with reference to Figure 1, when $j = 1$ we let $j - 1 = 4$. The symbols b, f and n represent functional relationships, which are specified in the cited reference or else are trivial, as is the case of Eq. 19. When the external stream is leaving the unit, i.e., it is either the extract or the raffinate; Eqs. 18 and 19 reduce to $\boldsymbol{E}_j = \boldsymbol{F}^i_j = \boldsymbol{F}^o_{j-1}$.

The system of Eqs. 15 to 20 constitute a system of nonlinear algebraic equations that can be solved numerically for any given set of operating conditions. From the states of the different streams, the separation performance of the unit can be calculated in terms of any desired performance parameter, such as purity and recovery (cf. Storti et al., 1995).

Operating Conditions to Achieve Complete Separation

The space spanned by the operating parameters m_j, $j = 1, \ldots, 4$, has been analyzed through a trial and error numerical procedure to determine the complete separation region.

The data and pictures that will be reported in this section are the results of parametric calculations performed using values of the relevant quantities which are representative of systems of practical interest. In some cases the values have been chosen in order to show some characteristic features of the behavior of systems described by the nonstoichiometric Langmuir isotherm.

In the following, all the different unit configurations of a TCC (or the equivalent SMB) adsorptive separation unit are first described and the constraints on the operating conditions of the two sections used to regenerate the adsorbent and the desorbent, namely sections 1 and 4, are discussed. Then, different examples are considered with the objective of showing on one hand the peculiarities of the complete separation region of the systems described in this work with respect to stoichiometric systems. On the other hand, proper parametric calculations allow to demonstrate that the limiting procedures discussed when dealing with Eq. 6 reduce the nonstoichiometric behavior to either the linear or the stoichiometric ones. The role of parameters such as desorbent adsorptivity and feed composition will be examined in detail.

For the sake of simplicity, all the examples refer to binary feeds. The most and the least adsorbable components of the mixture to be separated are referred to as A and B, respectively, whereas the desorbent is called D. The extension of these results to multicomponent systems is straightforward.

Unit configuration

In the following sections we will present and discuss results concerning the projection of the region of complete separation onto the (m_2, m_3) plane. The motivation for this is that in an adsorptive countercurrent separation unit sections 2 and 3 play the key role of performing the separation with operating conditions which are tightly coupled. On the other hand, the role of sections 1 and 4 is to regenerate the adsorbent and the desorbent, respectively, in order to make their recycle possible.

In this context it is worth noting that if the recycle of the desorbent is not desired or convenient, section 4 can be eliminated and pure desorbent is directly fed to section 1, whereas regenerated adsorbent is recycled to section 3. This modification of the classical four-section configuration in Figure 1 yields the three-section configuration illustrated in Figure 4. This has been used in several applications (cf., Ruthven and Ching, 1989; Baciocchi et al., 1996). In principle, also section 1 can be eliminated in those cases where there is no need to recycle the adsorbent. A two-section configuration is obtained, where fresh adsorbent is continuously fed to the second section of the unit. The practical interest of this last solution refers to processes where the adsorbent is regenerated off-line with respect to the separation process itself (cf. Ruthven and Ching, 1989).

Operating conditions in sections 1 and 4

To the aim of performing their specific tasks, the constraints on the operating conditions in sections 1 and 4 are in principle simple: flow rate ratios m_1 and m_4 must be high and low enough, respectively. The bound on the value of m_1 can be obtained by recalling that the constant state prevailing at steady state in section 1 must be pure desorbent. To achieve this, the term $m_1\delta_1$ must be greater than $\rho_f\gamma_{max}/\Gamma^\infty$, where δ_1 is calculated at the composition of the steady constant state prevailing inside the section 1 and γ_{max} corresponds to the most adsorbable component of the feed stream. This condition is necessary and sufficient if the desorbent is not strong, i.e., more adsorbable than all the components of the feed mixture. Since the state inside section 1 is pure desorbent, the relationship $\delta_1 = 1 + K_D c_D = 1 + K_D \rho_f$ holds true (cf. Eq. 7), and the following bound on m_1 is obtained:

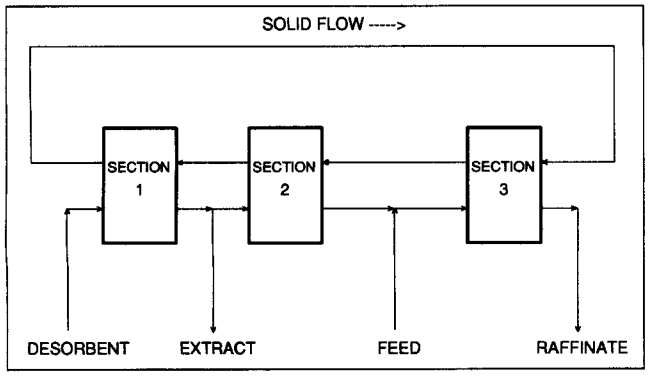

Figure 4. Three-section open-loop true countercurrent unit for adsorption separation.

$$m_1 > \frac{\rho_f \gamma_{max}}{\Gamma^\infty(1 + K_D \rho_f)}; \tag{21}$$

Notice that this bound is independent of the flow rate ratios in the other sections of the unit.

In the case of strong desorbent the bound on m_1 depends on m_2, m_3 and m_4 (cf. Part 2). However, a conservative upper value can be found as in the case of stoichiometric systems (see Appendix B of Part 2), yielding the following constraint, which is independent of the other flow rate ratios:

$$m_1 > \frac{\rho_f \Gamma_D^\infty K_D}{\Gamma^\infty(1 + K_D \rho_f)}. \tag{22}$$

For every value of desorbent adsorptivity, the bound on the value of m_4 is not explicit, i.e., it is dependent on the other flow rate ratios: $m_4 < m_{4,cr}(m_1, m_2, m_3)$. However, if the desorbent is weak, an independent conservative lower bound can be found, as follows:

$$m_4 < \frac{\rho_f \Gamma_D^\infty K_D}{\Gamma^\infty(1 + K_D \rho_f)}. \tag{23}$$

In the case where the desorbent is nonadsorbable the constraint (Eq. 21) on m_1 reduces to $m_1 > \rho_f\gamma_{max}/\Gamma^\infty$, whereas m_4 must fulfill the constraint (Eq. 24). An important special case (cf. the Appendix) is to separate a binary mixture using a nonadsorbable desorbent. In this case, the constraint on m_4 is:

$$m_4 < \frac{\rho_f}{2\Gamma^\infty}\left\{\gamma_{min} + m_3 + K_B c_B^F (m_3 - m_2) - \sqrt{[\gamma_{min} + m_3 + K_B c_B^F (m_3 - m_2)]^2 - 4\gamma_{min} m_3}\right\} \tag{24}$$

where γ_{min} corresponds to the weak component of the feed stream.

Thus summarizing, the complete separation regions derived in the following are constituted of points corresponding to operating conditions which in the frame of Equilibrium Theory guarantee the achievement of complete separation provided that the above constraints on m_1 and m_4 are fulfilled. Since these constraints are meant to realize complete regeneration of both the adsorbent and the desorbent in the four-section unit, they allow to reach conditions equivalent to those achieved in a three-section configuration where fresh desorbent is fed to the unit and in a two-section configuration where also fresh adsorbent is continuously fed. Therefore, the complete separation regions in the (m_2, m_3) plane that will be discussed in the following apply to all the unit configurations discussed so far, i.e., two-, three- and four-section configurations, provided that the above constraints on the remaining sections, if any, are fulfilled.

Regions of separation

Let us refer to a model system, whose parameters are summarized in the caption of Figure 5, where the different regions of separation in the (m_2, m_3) plane are illustrated. In comparison with Figure 2, it can be noted that the topologi-

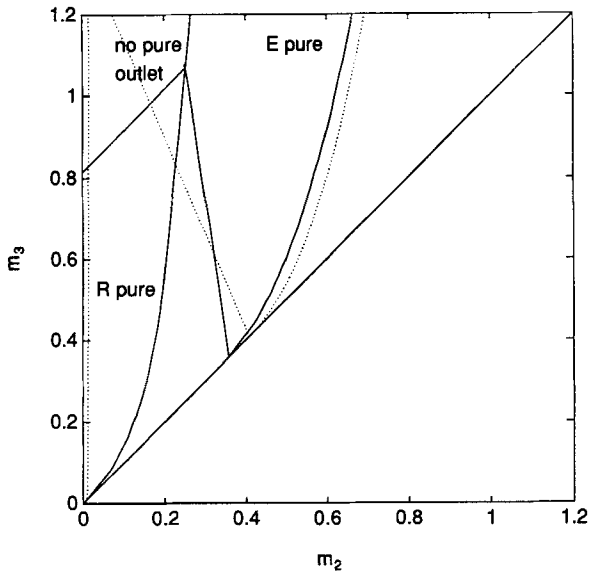

Figure 5. Regions of the (m_2, m_3) plane with different separation regimes in terms of purity of the outlet streams.

— Nonstoichiometric Langmuir isotherm: $\Gamma_A^\infty = 0.85$ mol/kg, $\Gamma_B^\infty = 0.03$ mol/kg, $\Gamma_D^\infty = 0.7$ mol/kg, $\Gamma^\infty = 0.8$ mol/kg; $K_A = 9.1$ m^3/mol, $K_B = 3.0$ m^3/mol, $K_D = 27$ m^3/mol, $\rho_f = 100$ mol/m^3, $y_A^F = 0.3$, $y_B^F = 0.7$. ····· Stoichiometric Langmuir isotherm: $K_A = 1$, $K_B = 0.012$, $K_D = 2.5$, $y_A^F = 0.3$, $y_B^F = 0.7$.

cal structure of these regions is the same in the two cases. However, when comparing the nonstoichiometric region with the one drawn with broken lines in Figure 5, which refers to a stoichiometric system with the same selectivities between the three species involved and an average value for the saturation loading capacity, a significant quantitative difference is observed. This indicates that a nonstoichiometric system cannot be approximated with a stoichiometric one by simply adjusting the parameters of the latter.

There is an important difference between the two equilibrium models, which is due to their different structure and should be pointed out. In the case of the stoichiometric isotherm (Eq. 5) the regions of separation depend on the equilibrium constants of all the species involved, on the saturation loading capacity and on the feed composition, whereas in the case of the nonstoichiometric isotherm (Eq. 6) they depend on the equilibrium constant and the saturation loading capacity of each component, on the feed composition, and also on the overall fluid-phase concentration. Therefore, for a given separation where the feed composition is given once and for all, in the stoichiometric case all the information about the operating conditions are accounted for through the parameters m_j but do not have any impact on the position of the complete separation region. On the contrary, in the nonstoichiometric case if there is a change, for example, in the operating temperature or pressure, so as to modify the fluid-phase density, then not only the flow rates m_j are changed but also the complete separation region is modified.

These preliminary results provide motivation for a deeper investigation on the differences and the analogies between the stoichiometric and the nonstoichiometric behavior with respect to the calculated regions of complete separation in the (m_2, m_3) plane.

Role of the nonstoichiometric character of the isotherm

In order to deepen this point the complete separation regions drawn in Figures 6 and 7 have been calculated. In both cases the idea is that of starting from a reference case, indicated by the letter (a) in the figures, where all components have the same saturation loading capacities. Then, for only one of the three components of the system the values of K_i and Γ_i^∞ are changed while keeping the same values of the selectivities between the different species, i.e., the same value of the parameter $\gamma_i = K_i\Gamma_i^\infty$. The parameters of the other two components are left unchanged. In Figure 6 the parameters of the desorbent, which in this case has an intermediate adsorptivity with respect to the two components to be separated, are modified, whereas in Figure 7 the parameters of the less adsorbable component in the feed mixture, i.e., component B, are changed.

In both cases very different complete separation regions are obtained, thus proving that accounting for different values of the saturation loading capacities is of key importance in predicting the behavior of adsorptive separation units.

Let us now consider the intersection points between the boundaries of the complete separation region and the straight line $m_3 = m_2$. Since the difference $(m_3 - m_2)$ is proportional to the feed flow rate, points close to the straight line $m_3 = m_2$ correspond to operations where the feed flow rate is very small with respect to the desorbent flow rate so that the components to be separated are very diluted inside the unit. Under these conditions the parameter δ_{LNS} can be approximated by $\delta_{LNS} = 1 + K_D c_D$, where c_D is very close to the overall concentration of the fluid phase ρ_f. Therefore, the dimensionless adsorbed phase concentration of components A and B given by Eq. 6 depends linearly on their fluid-phase

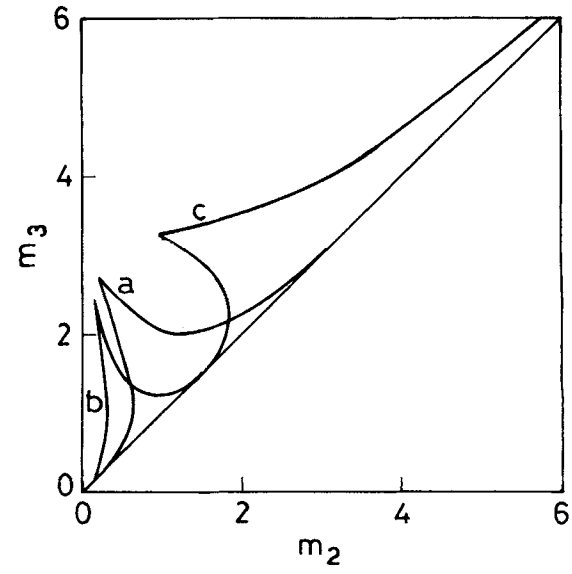

Figure 6. Role of the nonstoichiometric character of the isotherm.

Regions of complete separation in the (m_2, m_3) plane for equal binary selectivities but different adsorption equilibrium constant of the desorbent. $\Gamma_A^\infty = 0.2$ mol/kg, $\Gamma_B^\infty = 0.2$ mol/kg, $\Gamma^\infty = 0.2$ mol/kg, $K_A = 10$ m^3/mol, $K_B = 1.0$ m^3/mol, $\rho_f = 95$ mol/m^3, $y_A^F = 0.3$, $y_B^F = 0.7$. (a) $K_D = 3$ m^3/mol, $\Gamma_D^\infty = 0.2$ mol/kg; (b) $K_D = 6$ m^3/mol, $\Gamma_D^\infty = 0.1$ mol/kg; (c) $K_D = 1$ m^3/mol, $\Gamma_D^\infty = 0.6$ mol/kg.

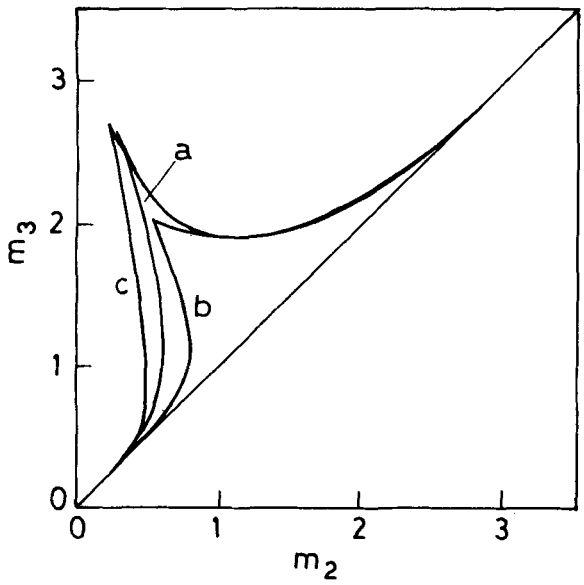

Figure 7. Role of the nonstoichiometric character of the isotherm.

Regions of complete separation in the (m_2, m_3) plane for equal binary selectivities but different adsorption equilibrium constant of the weak component. $\Gamma_A^\infty = 0.2$ mol/kg, $\Gamma_D^\infty = 0.2$ mol/kg, $\Gamma^\infty = 0.2$ mol/kg, $K_A = 10$ m^3/mol, $K_D = 3$ m^3/mol, $\rho_f = 95$ mol/m^3, $y_A^F = 0.3$, $y_B^F = 0.7$. (a) $K_B = 1$ m^3/mol, $\Gamma_B^\infty = 0.2$ mol/kg; (b) $K_B = 4$ m^3/mol, $\Gamma_B^\infty = 0.05$ mol/kg; (c) $K_B = 0.5$ m^3/mol, $\Gamma_B^\infty = 0.4$ mol/kg.

concentration, being the proportionality constant (i.e., Henry constant) equal to $h_i = (\Gamma_i^\infty/\Gamma^\infty)\rho_f K_i/(1 + K_D \rho_f)$, with $i = A$, B. It follows that near the straight line $m_3 = m_2$ the complete separation region tends to resemble that of a linear system. It is known that the coordinates of the intersection points of the boundaries of the complete separation region for a linear system are given exactly by the constants h_A and h_B. These values are decreasing functions of the equilibrium constant of the desorbent K_D, hence they do not change in Figure 7 where neither K_D nor the numerator of the parameter h_B change. On the contrary K_D is modified in the examples of Figure 6 together with Γ_D^∞, hence the parameters h_A and h_B do change and the complete separation regions are shifted in the plane (m_2, m_3).

In Figure 7, where γ_B and the selectivity between the two components to be separated $S_{AB} = \gamma_A/\gamma_B$ remain constant, (A stronger than B) it is observed that higher values of the equilibrium constant of the weak component K_B correspond to smaller complete separation regions. This indicates that the apparent selectivity decreases, i.e., that the apparent adsorptivity of component B increases.

The same effect can be observed in Figure 6 by noticing that in all the three cases γ_D remains constant and the sides of the triangle shaped complete separation regions are both curved and tailed. This feature is typical of systems where the desorbent is intermediate and it is further exemplified in Figure 11. Note in the latter figure that in the case of weak or strong desorbent the lefthand or righthand side, respectively, of the triangle shaped region consists of a straight line. Moreover, with reference to region (a), by increasing the value of K_D the complete separation region is shifted towards the left as if the desorbent were now a strong desorbent. Accordingly when K_D decreases, the complete separation region is shifted toward the right, and acquires the weak desorbent characteristic long right tail. Also these effects should be compared with the examples shown in Figure 11.

Thus to sum up, also in the case of Figure 6 a change in the equilibrium constant value yields a change in the apparent adsorptivity of the desorbent. This can be justified by recalling that in Eq. 6 the equilibrium constant K_i appears not only in the numerator, where it is coupled with the saturation loading capacity Γ_i^∞, but also in the denominator. Therefore, the two parameters play a coupled role in determining the component adsorptivity and its selectivity with respect to the other components as indicated by Eq. 8, but the individual values are also important in determining the behavior of the system as demonstrated by the results shown in Figures 6 and 7.

Linear behavior at low fluid-phase concentration

When discussing Eq. 6, it was underlined that a linear system can be seen as the limit model of a nonstoichiometric system at very high dilution. This feature of the two models can be observed also in terms of complete separation regions in the (m_2, m_3) plane. This is illustrated in Figure 8, where for a separation with given selectivities, the complete separation regions for different values of the overall fluid-phase density ρ_f obtained using the nonstoichiometric model are shown (for the sake of simplicity also the reference value of the adsorbed phase reference concentration Γ^∞ has been

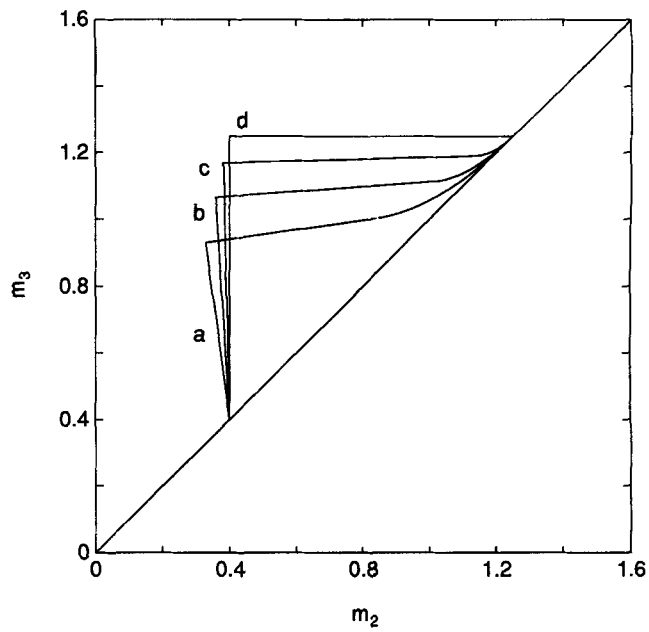

Figure 8. Role of the fluid phase concentration: linear behavior at high dilution.

Regions of complete separation in the (m_2, m_3) plane for equal selectivities but different fluid-phase concentration. $\Gamma_A^\infty = 0.25$ mol/kg, $\Gamma_B^\infty = 0.2$ mol/kg, $\Gamma_D^\infty = 0$ mol/kg, $K_A = 0.5$ m^3/mol, $K_B = 0.2$ m^3/mol, $K_D = 0$ m^3/mol, $y_A^F = 0.5$, $y_B^F = 0.5$. (a) $\rho_f = 1$ mol/m^3, $\Gamma^\infty = 0.1$ mol/kg; (b) $\rho_f = 0.5$ mol/m^3, $\Gamma^\infty = 0.05$ mol/kg; (c) $\rho_f = 0.2$ mol/m^3, $\Gamma^\infty = 0.02$ mol/kg; (d) linear isotherm: $H_A = 1.25$, $H_B = 0.4$. Notice that a nonadsorbable desorbent has been considered: in this case the boundaries of the complete separation region can be calculated following the procedure reported in the Appendix.

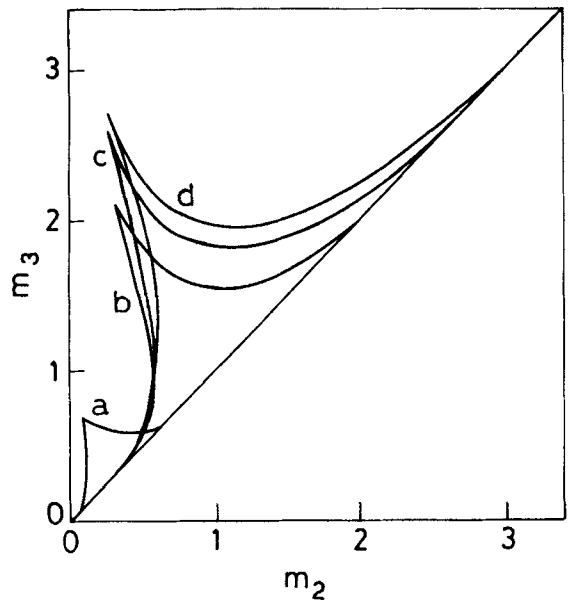

Figure 9. Role of the adsorptivity of the fluid species: stoichiometric behavior at high adsorptivity.

Regions of complete separation in the (m_2, m_3) plane for equal binary selectivities and saturation loading capacities but different values of the adsorption equilibrium constants. $\Gamma_A^\infty = 0.2$ mol/kg, $\Gamma_B^\infty = 0.2$ mol/kg, $\Gamma_D^\infty = 0.2$ mol/kg, $\Gamma^\infty = 0.2$ mol/kg, $\rho_f = 95$ mol/m^3, $y_A^F = 0.3$, $y_B^F = 0.7$. (a) $K_A = 10 \times 10^{-3}$ m^3/mol, $K_B = 1 \times 10^{-3}$ m^3/mol, $K_D = 3 \times 10^{-3}$ m^3/mol; (b) $K_A = 10 \times 10^{-2}$ m^3/mol, $K_B = 1 \times 10^{-2}$ m^3/mol, $K_D = 3 \times 10^{-2}$ m^3/mol; (c) $K_A = 10 \times 10^{-1}$ m^3/mol, $K_B = 1 \times 10^{-1}$ m^3/mol, $K_D = 3 \times 10^{-1}$ m^3/mol; (d) $K_A = 10$ m^3/mol, $K_B = 1$ m^3/mol, $K_D = 3.0$ m^3/mol. Region (d) overlaps entirely the complete separation region calculated for the stoichiometric Langmuir isotherm using the following parameters: $K_A = 10$, $K_B = 1$, $K_D = 3$, $y_A^F = 0.3$, $y_B^F = 0.7$.

changed). The complete separation region calculated for the linear model obtained by letting $\delta = 1$ in Eq. 6 is also shown. As expected when ρ_f decreases, the complete separation region calculated using the nonstoichiometric model approaches that obtained using the linear model.

Stoichiometric behavior at high adsorptivity

Let us consider a system described by a nonstoichiometric Langmuir isotherm with the same value of the saturation loading capacity for all components, i.e., $\Gamma_i^\infty = \Gamma^\infty$ for $i = A, B, D$. Different calculations have been performed for the same values of the selectivities but different values of the equilibrium constants K_i, $i = A, B, D$. As discussed with reference to Eq. 6, by increasing the values of the equilibrium constants, hence the values of the adsorptivity γ_i of the components of the fluid mixture, this system approaches the behavior of the corresponding stoichiometric system. This property of the two equilibrium models is illustrated in Figure 9 in terms of the different regions of complete separation. When the values of K_i are increased several orders of magnitude in a proprotional manner for all components, the region of complete separation approaches that calculated with the stoichiometric model, which in this case corresponds almost exactly to the last one calculated using the nonstoichiometric model and it cannot be distinguished in the figure. Note that a similar behavior could have been observed by letting the

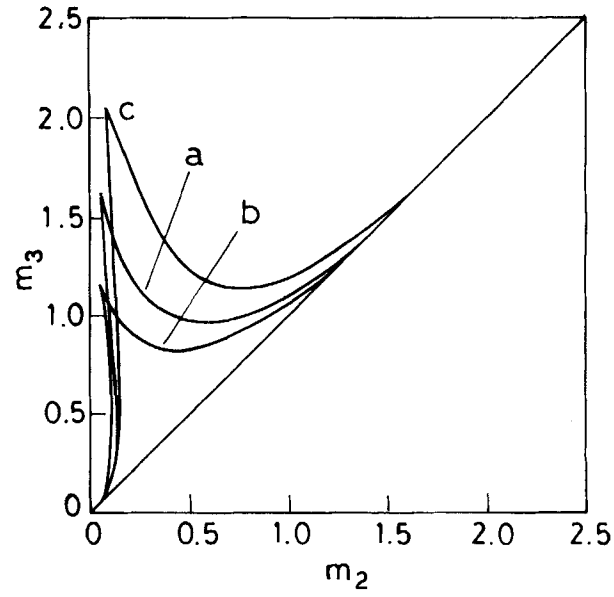

Figure 10. Effect of feed composition changes on the region of complete separation in the (m_2, m_3) plane.

$\Gamma_A^\infty = 0.85$ mol/kg, $\Gamma_B^\infty = 0.03$ mol/kg, $\Gamma_D^\infty = 0.14$ mol/kg, $\Gamma^\infty = 0.8$ mol/kg, $K_A = 9.1$ m^3/mol, $K_B = 3$ m^3/mol, $K_D = 6$ m^3/mol, $\rho_f = 95$ mol/m^3. (a) $y_A^F = 0.5$, $y_B^F = 0.5$; (b) $y_A^F = 0.7$, $y_B^F = 0.3$; (c) $y_A^F = 0.3$, $y_B^F = 0.7$.

values of K_i constant and increasing the overall fluid phase density ρ_f.

Role of feed composition

In the previous paragraphs the differences between the nonstoichiometric and the stoichiometric behavior have been investigated so as to stress the peculiar features of systems described by the nonstoichiometric Langmuir isotherm. However, from a qualitative point of view systems described by these two adsorption isotherms show remarkable similarities. In particular, this is evident when certain characteristic effects are considered.

First we deal with the role of feed composition. In terms of the region of complete separation in the (m_2, m_3) plane the obtained results are illustrated in Figure 10, where three examples are considered with an A/B ratio in the feed stream equal to 70/30, 50/50 and 30/70, all the other parameters remaining the same. In all cases the basis of the triangle shaped complete separation region, i.e., its intersection with the straight line $m_3 = m_2$, remains the same. On the contrary, the vertex of the triangle, which is the optimal point for the separation, moves from the lower left, when the concentration of the more adsorbable component A is higher, to the upper right when it is lower. This qualitative behavior is similar and consistent with that exhibited by stoichiometric systems (cf. Storti et al., 1993a; Mazzotti et al., 1994).

Role of desorbent adsorptivity

The effect of desorbent adsorptivity on the shape and location of the complete separation region is illustrated in Figure 11. Here there are complete separation regions for the same

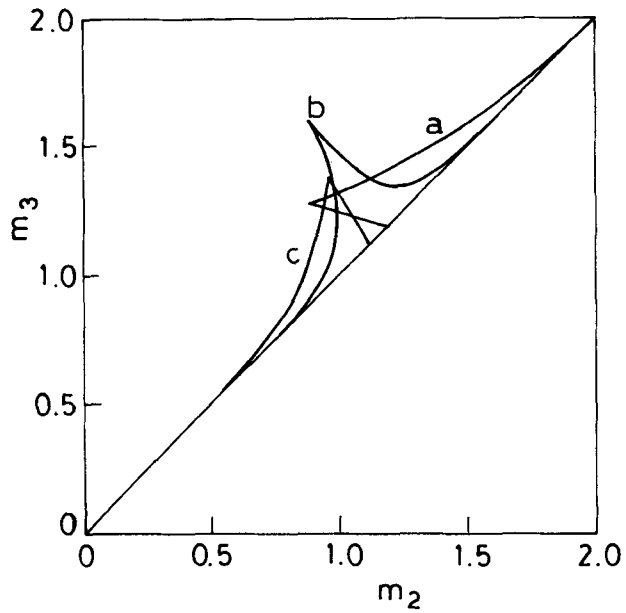

Figure 11. Effect of desorbent adsorptivity on the region of complete separation in the (m_2, m_3) plane.

$\Gamma_A^\infty = 0.25$ mol/kg, $\Gamma_B^\infty = 0.2$ mol/kg, $\Gamma^\infty = 0.2$ mol/kg, $K_A = 1.8$ m^3/mol, $K_B = 1.2$ m^3/mol, $\rho_f = 95$ mol/m^3, $y_A^F = 0.5$, $y_B^F = 0.5$. (a) Weak desorbent: $\Gamma_D^\infty = 0.1$ mol/kg, $K_D = 1$ m^3/mol; (b) intermediate desorbent: $\Gamma_D^\infty = 0.25$ mol/kg, $K_D = 1.5$ m^3/mol; (c) strong desorbent: $\Gamma_D^\infty = 0.3$ mol/kg, $K_D = 2$ m^3/mol.

binary separation, i.e., same feed composition and same values of the adsorption parameters (K_i and Γ_i^∞ for A and B), but for different values of the desorbent adsorptivity, i.e., different values of the term $\gamma_D = K_D\Gamma_D^\infty$. It can readily be observed that in the case of weak desorbent higher values of the flow rate ratios m_2 and m_3 than in the case of intermediate desorbent are required to achieve complete separation for the same value of the difference $(m_3 - m_2)$, i.e., for the same feed flow rate. On the contrary, when the desorbent is strong, lower values of m_2 and m_3 than in the case of intermediate desorbent are needed.

This result compares well with what was obtained when dealing with stoichiometric systems (cf. Mazzotti et al., 1994). However, the following noteworthy difference arises in this case. In the former case only three adsorption parameters are available, namely the equilibrium constants K_A, K_B and K_D; therefore, in order to study the role of desorbent adsorptivity it is enough to consider three cases: where K_D is lower than K_B, where K_D is intermediate between K_B and K_A and finally where K_D is greater than K_A. Provided that these inequalities are fulfilled the specific values of the parameters that have been chosen do not modify the overall qualitative picture. On the contrary, in the nonstoichiometric case the parameters are six: the saturation loading capacities Γ_A^∞, Γ_B^∞ and Γ_D^∞ in addition to the equilibrium constants mentioned above. In choosing the equilibrium parameters for the components A and B a rather arbitrary choice of the saturation loading capacities has been made. When considering the results illustrated in Figure 7, it is rather evident that a different choice would produce rather different complete separation regions with respect to those reported in Figure 11. However, this does not alter the general behavior outlined above.

Experimental Results

In order to validate the theoretical results obtained above for a countercurrent unit, we now compare them with the experimental performance of a simulated moving bed unit. For this we use the conversion rules between SMB and TCC units, based upon their kinematic equivalence

$$\frac{L}{t^*} = \frac{u_s}{1-\epsilon} \tag{25}$$

$$G_j = A\rho_f[u_j + u_s\epsilon/(1-\epsilon)]. \tag{26}$$

Thus, the flow rate ratio parameters m_j defined by Eq. 4 for TCC units, in the case of a SMB configuration become

$$m_j = \frac{G_j t^* - AL\epsilon^*\rho_f}{AL\rho_s\Gamma^\infty(1-\epsilon^*)} \quad (j = 1, \ldots, 4). \tag{27}$$

We see that m_j accounts for all the operating parameters typical of a SMB unit, i.e., the fluid molar flow rate G_j, the switching time t^*, the cross section A and length L of each column, and the involved physical properties. Let us consider a set of experimental runs performed in a six port simulated moving bed pilot plant operated in the vapor phase having a feed stream constituted of 70% *iso*-pentane and 30% *n*-pentane, with *n*-heptane as desorbent and 5A-zeolite as adsorbent (Baciocchi et al., 1996). The relevant operating conditions and physico-chemical data are summarized in Table 1 (the adsorption equilibrium parameters have been evaluated by Mazzotti et al., 1996). The reported value of the fluid-phase molar density ρ_f corresponds to the average value among those observed in the different runs. Notice that for the separation under examination the desorbent adsorptivity is greater than those of the two components to be separated, of which *n*-pentane is more adsorbable.

Figure 12 represents the points corresponding to the operating conditions adopted in the experimental runs located in

Table 1. Separation of *n*- and *iso*-Pentane: Physicochemical Data and Operating Conditions of Experimental Runs

Equilibrium Parameters	
$\Gamma_{i-C_5}^\infty$	0.03 mol/kg
$\Gamma_{n-C_5}^\infty$	0.85 mol/kg
$\Gamma_{n-C_7}^\infty$	0.7 mol/kg
Γ^∞	0.8 mol/kg
K_{i-C_5}	3.0 m^3/mol
K_{n-C_5}	9.1 m^3/mol
K_{n-C_7}	27 m^3/mol
Operating temperature	448 K
Operating pressure	350 kPa
ρ_f	100 mol/m^3
Feed composition	$y_{i-C_5}^F = 0.7$, $y_{n-C_5}^F = 0.3$
ϵ	0.30
ϵ_p	0.33
ρ_s	1,665 kg/m^3
A	1.767×10^{-4} m^2
L	1 m
t^*	180 s
Unit configuration	2-2-2

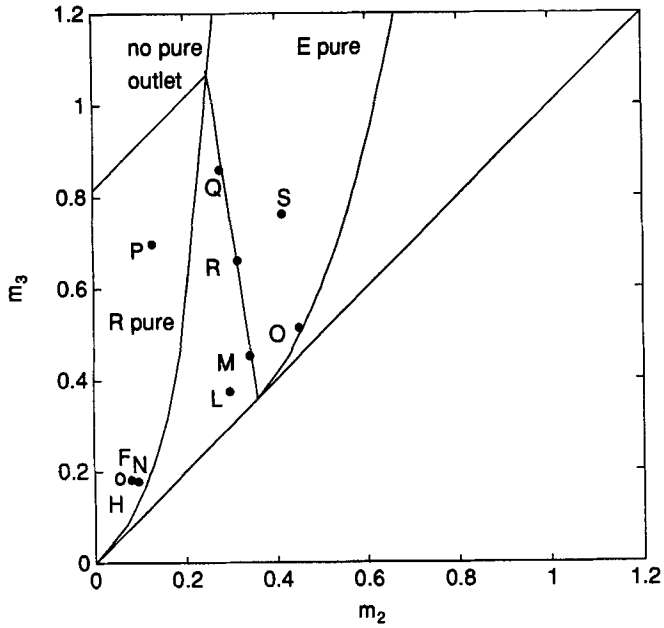

Figure 12. Separation of *n*- and *iso*-pentane (Baciocchi et al., 1996): relative position of the experimental operating points (●) in the (m_2, m_3) plane with respect to the calculated regions of separation.

Point F (○) is the only one for which the constraint on m_1 is not fulfilled. Equilibrium parameters, operating conditions and measured separation performances are reported in Tables 1 and 2.

the (m_2, m_3) plane together with the regions of separation calculated through the procedure discussed in this article using the parameters in Table 1. The values of the parameters m_j for these experimental runs calculated through Eq. 27 are summarized in Table 2. Note that in calculating the values of the parameters m_j the observed values of the fluid-phase molar density in each experiment have been used: the difference among these and the average value reported in Table 1 is always less than 10%. In Table 2 the experimental values of the separation performance parameters are also reported: purity in the extract stream (i.e., the mole percentage of *n*-pentane in the extract with respect to the desorbent free overall concentration) and purity in the Raffinate stream (i.e., the mole percentage of *iso*-pentane in the raffinate with respect to the desorbent free overall concentration).

Table 2. Separation of *n*- and *iso*-pentane: Flow Rate Ratios and Separation Performances of Experimental Runs*

	Flow Rate Ratios				Experimental Purity Values	
Run	m_1	$(m_{1,cr})$	m_2	m_3	P_E (%)	P_R (%)
F	0.419	(0.386)	0.042	0.166	14	12
H	0.632	(0.377)	0.082	0.170	38	100
L	0.622	(0.395)	0.297	0.361	100	100
M	0.638	(0.422)	0.336	0.427	100	100
N	0.628	(0.373)	0.095	0.166	38	100
O	0.675	(0.450)	0.454	0.503	100	79
P	0.707	(0.502)	0.137	0.692	74	100
Q	0.703	(0.530)	0.280	0.838	100	99
R	0.695	(0.489)	0.321	0.645	100	100
S	0.722	(0.520)	0.418	0.751	100	95

*Critical value of the flow rate ratio in section 1, $m_{1,cr}$, is reported between parentheses aside the operating value, m_1.

By considering the relative position of the operating points with respect to the predicted regions of separation shown in Figure 12, it can readily be observed that for all of them but two the location in the operative plane is in agreement with the experimental purities reported in Table 2. In particular, as expected on the basis of the observed experimental performance points H, N and P are in the pure raffinate region, points O and S belong to the pure extract region, while points L, M and R fall inside the complete separation triangle.

Of the two exceptions mentioned above, the first one refers to run Q, whose corresponding operating point is in the complete separation region, whereas a very small amount of *n*-pentane has been measured in the raffinate, thus yielding only 99% purity. This can be explained by noticing that point Q is very close to the vertex of the triangle and to the boundary with the pure extract region. In this location the separation performance, and particularly the raffinate purity, is expected to be rather sensitive to experimental disturbances or model uncertainties.

The result of the experimental run F constitutes the second apparent disagreement with the theory. The clue here is in fact that the flow rate ratio m_1 in this case is too small so that the adsorbent is not completey regenerated in section 1. Thus, as discussed above, the analysis based on the separation regions in the (m_2, m_3) plane does not apply. By inspection of the data in Table 2, it is readily seen that m_1 in run F is smaller than in all the other experimental runs. The evaluation of the critical m_1 value for each run is not straightforward and involves a one-dimensional numerical search on the straight line spanned by the parameter m_1. The obtained values are reported between parentheses for each run in Table 2. It can be observed that in all the experimental runs, including run F, the operating parameter m_1 is greater than the corresponding critical value. However, run F is the only one where the value of m_1 is only 10% larger than the critical value. In these conditions, experimental disturbances and model uncertainties play an important role and hinder the predicted separation performance. It is worth noting that the upper bound given by Eq. 23 in this case is of no help since by using the parameter values in Table 1 it leads to an excessively conservative value of 0.875, which would erroneously indicate that m_1 is lower than the critical value in all the experimental runs.

Conclusion

In view of the increasing importance of the adsorptive separation processes of multicomponent mixtures through the simulated moving bed technology, it is important to develop methods for the optimal design of their operating conditions to achieve the desired separation performance. These have been developed in this work in the frame of equilibrium theory and with reference to systems characterized by the nonstoichiometric Langmuir isotherm. The differences among these and stoichiometric and linear systems, which have been considered in previous works, are discussed in detail. In particular, a thorough analysis of the assumption of constant fluid-flow rate in the case of these three adsorption equilibrium models has been reported.

The design of the operating conditions is performed by de-

termining the complete separation region in the operating parameter space, whose coordinates are the flow rate ratios m_j in each section of the separation unit. This region is constituted of points that correspond to operating conditions which allow complete separation.

In particular, it is shown that the operating conditions in the two sections of the unit where the desorbent and the adsorbent are regenerated, namely sections 4 and 1, respectively, are relatively simple. Therefore, a given separation is best analyzed by considering the projection of the complete separation region in the (m_2, m_3) plane. This geometrical representation allows to elucidate the role of the different operating parameters in determining the separation performance.

The outcome of the analysis is twofold: on the first hand nonstoichiometric systems exhibit important quantitative differences with respect to stoichiometric systems, thus demonstrating that a richer equilibrium description, such as the one offered by the latter isotherm with respect to the former, is of key importance in characterizing the separation performance of countercurrent adsorptive separation units. On the other hand, the overall behavior of nonstoichiometric systems is qualitatively similar to that exhibited by stoichiometric systems, in particular in terms of the role and effect of such parameters as feed composition and desorbent adsorptivity. These findings allow us to extend directly all the concepts and criteria developed in previous works to design robust and optimal operating conditions of countercurrent separation units to systems characterized by the nonstoichiometric Langmuir isotherm (cf. Storti et al., 1995).

The reliability and accuracy of the theoretical findings presented in this work have been assessed by comparison with a set of experimental results. These have been obtained in a six port SMB pilot unit, operated in the vapor phase using a three-section open-loop configuration. The study case considered is the separation of linear and nonlinear paraffins, using 5A-Zeolite as adsorbent.

Acknowledgments

The first and second part of this series were presented by Storti et al. (1993a) and Mazzotti et al. (1994). We gratefully acknowledge the financial support of CNR Progetto Finalizzato Chimica Fine II.

Notation

A = cross section of the adsorption column
A_j = state of the solid stream in section j
c_i = fluid phase molar concentration of component i
f_i^j = dimensionless net flow rate of component i in section j, $f_i^j = m_j y_i^j - \theta_i^j$
F_j = state of the fluid stream in section j
L_j = length of section j in a TCC unit
P_E = desorbent free extract purity
P_R = desorbent free raffinate purity
s = parameter defined by Eq. 11
S_{il} = selectivity between components i and l
S_j = constant state prevailing in section j
u_s = superficial solid phase velocity
x = dimensionless axial coordinate, $x = z/L_j$
y_i = fluid-phase dimensionless concentration of component i, $y_i = c_i/\rho_f$
z = axial coordinate

Greek letters

β_i = modified adsorptivity of component i, $\beta_i = \gamma_i \rho_f/\Gamma^\infty$
γ_i = adsorptivity of component i, $\gamma_i = K_i\Gamma_i^\infty$
Γ_i = adsorbed phase molar concentration of component i
δ = denominator in the Langmuir isotherm, Eq. 6
ϵ = external void fraction
ϵ_p = intraparticle void fraction
ϵ^* = overall void fraction, $\epsilon^* = \epsilon + \epsilon_p(1-\epsilon)$
θ_i = adsorbed phase dimensionless concentration of component i, $\theta_i = \Gamma_i/\Gamma^\infty$
Θ = total coverage of the adsorbent
ρ_i = fluid phase molar density of component i
ρ_s = bulk solid mass density
σ = capacity ratio, $\sigma = \rho_s\Gamma^\infty/\rho_f$
τ = dimensionless time = tu_s/L
ω = equilibrium theory parameter defined by Eq. 9

Subscripts and superscripts

c = constant state in the column
cr = critical value of the operating parameter
F = feed
i = component index; also incoming stream in Figure 3
o = outgoing stream in Figure 3

Literature Cited

Baciocchi, R., M. Mazzotti, G. Storti, and M. Morbidelli, "C_5 Separation in a Vapor Phase Simulated Moving Bed Unit," *Fundamentals of Adsorption*, M. D. LeVan, ed., Kluwer Academic Publ., Boston, MA, p. 75 (1996).

Barrer, R. M., *Zeolites and Clay Minerals as Sorbents and Molecular Sieves*, Academic Press, London (1978).

Broughton, D. B., and C. G. Gerhold, "Continuous Sorption Process Employing Fixed Beds of Sorbent and Moving Inlets and Outlets," U.S. Patent 2,985,589 (May 23, 1961).

Ching, C. B., B. G. Lim, E. J. D. Lee, and S. C. Ng, "Preparative Resolution of Praziquantel Enantiomers by Simulated Counter-Current Chromatography," *J. Chromatog.*, **634**, 215 (1993).

Fish, B. B., R. W. Carr, and R. Aris, "The Continuous Countercurrent Moving Bed Separator," *AIChE J.*, **35**, 737 (1989).

Fish, B. B., R. W. Carr, and R. Aris, "Optimization of the Countercurrent Moving-Bed Chromatographic Separator," *AIChE J.*, **39**, 1621 (1993).

Filippov, L. K., "Coherent and Incoherent Frontal Patterns of Multicomponent Adsorption Dynamics for Variable Linear Fluid Velocity in the Fixed Bed: I. Frontal Patterns for Linear Adsorption Isotherms," *Chem. Eng. Sci.*, **49**, 3499 (1994).

Ganetsos, G., and P. E. Barker, "Semicontinuous Countercurrent Chromatographic Refiners," in *Preparative and Production Scale Chromatography*, G. Ganetsos and P. E. Barker, eds., Marcel Dekker, New York (1993).

Hashimoto, K., S. Adachi, Y. Shirai, and M. Morishita, "Operation and Design of Simulated Moving-Bed Adsorbers," *Preparative and Production Scale Chromatography*, G. Ganetsos and P. E. Barker, eds., Marcel Dekker, New York (1993).

Helfferich, F., and G. Klein, *Multicomponent Chromatography: Theory of Interference*, Marcel Dekker, New York (1970).

Johnson, J. A., and R. G. Kabza, "SORBEX: Industrial-Scale Adsorptive Separation," *Preparative and Production Scale Chromatography*, G. Ganetsos and P. E. Barker, eds., Marcel Dekker, New York (1993).

LeVan, M. D., C. A. Costa, A. E. Rodrigues, A. Bossy, and D. Tondeur, "Fixed-Bed Adsorption of Gases: Effect of Velocity Variations on Transition Types," *AIChE J.*, **34**, 996 (1988).

Mazzotti, M., R. Baciocchi, G. Storti, and M. Morbidelli, "Vapor-Phase SMB Adsorptive Separation of Linear/Nonlinear Paraffins," *Ind. Eng. Chem. Res.*, in press (1996).

Mazzotti, M., G. Storti, and M. Morbidelli, "Robust Design of Countercurrent Adsorption Separation Processes: 2. Multicomponent Systems," *AIChE J.*, **40**, 1825 (1994).

Negawa, M., and F. Shoji, "Optical Resolution by Simulated Moving-Bed Adsorption Technology," *J. Chromatog.*, **590**, 113 (1992).

Nicoud, R.-M., G. Fuchs, P. Adam, M. Bailly, E. Küsters, F. D. An-

tia, R. Reuille, and E. Schmid, "Preparative Scale Enantioseparation of a Chiral Epoxide: Comparison of Liquid Chromatography and Simulated Moving Bed Adsorption Technology," *Chirality*, **5**, 267 (1993).
Rhee, H.-K., R. Aris, and N. Amundson, "Multicomponent Adsorption in Continuous Countercurrent Exchangers," *Phil. Trans. Roy. Soc. London*, **A269**, 187 (1971).
Rhee, H.-K., R. Aris, and N. Amundson, *First-Order Partial Differential Equations*, Vol. II, Prentice-Hall Inc., Englewood Cliffs, NJ (1989).
Ruthven, D. M., *Principles of Adsorption and Adsorption Processes*, Wiley, New York (1984).
Ruthven, D. M., and C. B. Ching, "Counter-Current and Simulated Counter-Current Adsorption Separation Processes," *Chem. Eng. Sci.*, **44**, 1011 (1989).
Storti, G., R. Baciocchi, M. Mazzotti, and M. Morbidelli, "Design of Optimal Operating Conditions of Simulated Moving Bed Adsorptive Separation Units," *Ind. Eng. Chem. Res.*, **34**, 288 (1995).
Storti, G., M. Masi, S. Carrà, and M. Morbidelli, "Optimal Design of Multicomponent Adsorption Separation Processes Involving Nonlinear Equilibria," *Chem. Eng. Sci.*, **44**, 1329 (1989).
Storti, G., M. Mazzotti, L. T. Furlan, M. Morbidelli, and S. Carrà, "Performance of a Six Port Simulated Moving Bed Pilot Plant for Vapor-Phase Adsorption Separations," *Sep. Sci. Technol.*, **27**, 1889 (1992).
Storti, G., M. Mazzotti, M. Morbidelli, and S. Carrà, "Robust Design of Binary Countercurrent Adsorption Separation Processes," *AIChE J.*, **39**, 471 (1993a).
Storti, G., M. Mazzotti, L. T. Furlan, and M. Morbidelli, "Analysis of a Six Port Simulated Moving Bed Separation Unit," in *Fundamentals of Adsorption*, M. Suzuki, ed., Kodansha, Tokyo, p. 607 (1993b).

Appendix

Case of nonadsorbable desorbent

The complete separation regions reported in Figure 8 refer to the case of a binary separation where the desorbent is nonadsorbable, i.e., $K_D = \Gamma_D^\infty = 0$. This is clearly the particular case of a desorbent which is so weak that its adsorptivity is negligible (cf. for a practical application Fish et al., 1989, 1993). In this case the complete separation region may be calculated analytically following the procedure adopted earlier for the stoichiometric Langmuir isotherm. This is because also for this system the state of each stream exhibits a one-to-one mapping with a two-dimensional Ω space. For the sake of brevity, we do not report in detail the procedure to derive the explicit expressions for the boundaries of the complete separation region, since this is similar to that adopted earlier. The final result, with reference to Figure A1 is given by the following equations (notice that $\beta_i = \gamma_i \rho_f / \Gamma^\infty$)

- *Straight line wf*

$$[\beta_A - \omega_G(1 + K_A c_A^F)]m_2 + K_A c_A^F \omega_G m_3 = \omega_G(\beta_A - \omega_G) \tag{A1}$$

- *Straight line wb*

$$[\beta_A - \beta_B(1 + K_A c_A^F)]m_2 + K_A c_A^F \beta_B m_3 = \beta_B(\beta_A - \beta_B) \tag{A2}$$

- *Curve ra*

$$m_3 = m_2 + \frac{\left(\sqrt{\beta_A} - \sqrt{m_2}\right)^2}{K_A c_A^F} \tag{A3}$$

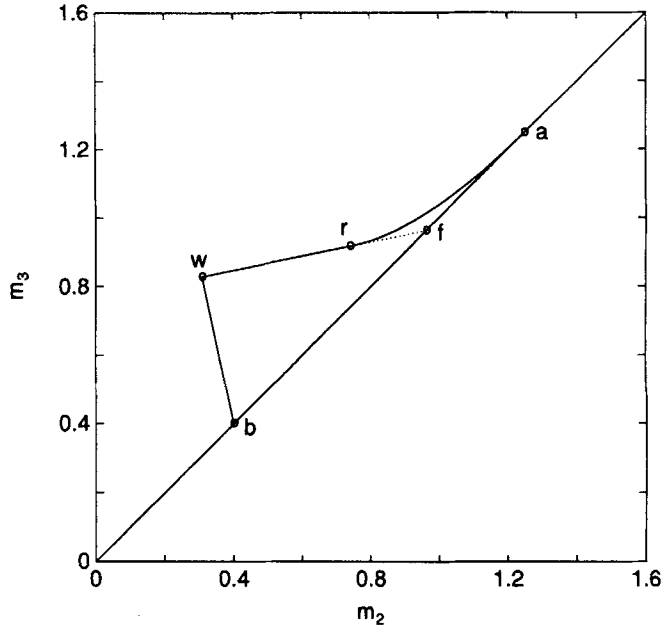

Figure A1. Region of complete separation in the (m_2, m_3) plane for a nonadsorbable desorbent.

$\Gamma_A^\infty = 0.25$ mol/kg, $\Gamma_B^\infty = 0.2$ mol/kg, $\Gamma^\infty = 0.15$ mol/kg, $K_A = 0.5$ m^3/mol, $K_B = 0.2$ m^3/mol, $\rho_f = 1.5$ mol/m^3, $y_A^F = 0.5$, $y_B^F = 0.5$.

- *Straight line ab*

$$m_3 = m_2 \tag{A4}$$

The coordinates of the intersection points are given by

point a (β_A, β_A) (A5)

point b (β_B, β_B) (A6)

point f (ω_G, ω_G) (A7)

point r

$$\left(\frac{\omega_G^2}{\beta_A}, \frac{\omega_G[\omega_F(\beta_A - \omega_G)(\beta_A - \beta_B) + \beta_B \omega_G(\beta_A - \omega_F)]}{\beta_A \beta_B(\beta_A - \omega_F)}\right) \tag{A8}$$

point w $$\left(\frac{\beta_B \omega_G}{\beta_A}, \frac{\omega_G[\omega_F(\beta_A - \beta_B) + \beta_B(\beta_B - \omega_F)]}{\beta_B(\beta_A - \omega_F)}\right) \tag{A9}$$

In the above equations ω_F and ω_G are the coordinates of the point corresponding to the feed state in the Ω space and are given by the roots of Eq. 9, which in this case reduces to

$$(1 + K_A c_A^F + K_B c_B^F)\omega^2 - [\beta_A(1 + K_B c_B^F) + \beta_B(1 + K_A c_A^F)]\omega + \beta_A \beta_B = 0. \tag{A10}$$

In particular, ω_F and ω_G correspond to the lower and upper root, respectively, hence $\omega_G > \omega_F > 0$.

Manuscript received Dec. 21, 1995, and revision received Mar. 28, 1996.